THE JOURNAL OF BIOLOGICAL CHEMISTRY VOL. 286, NO. 21, pp. 18692–18700, May 27, 2011

Multiple Peptide Resistance Factor (MprF)-mediated Resistance of *Staphylococcus aureus* against Antimicrobial Peptides Coincides with a Modulated Peptide Interaction with Artificial Membranes Comprising Lysyl-Phosphatidylglycerol*

Received for publication, February 3, 2011, and in revised form, April 6, 2011 Published, JBC Papers in Press, April 7, 2011, DOI 10.1074/jbc.M111.226886

Jörg Andrä[‡1], **Torsten Goldmann**[‡], **Christoph M. Ernst**[§], **Andreas Peschel**[§], **and Thomas Gutsmann**[‡]

From the [‡]*Research Center Borstel, Leibniz Center for Medicine and Biosciences, D-23845 Borstel, Germany and the* [§]*Cellular and Molecular Microbiology Division, Interfaculty Institute of Microbiology and Infection Medicine, University of Tübingen, 72074 Tübingen, Germany*

Modification of the membrane lipid phosphatidylglycerol (PG) of *Staphylococcus aureus* by enzymatic transfer of a L-lysine residue leading to lysyl-PG converts the net charge of PG from −1 to +1 and is thought to confer resistance to cationic antimicrobial peptides (AMPs). Lysyl-PG synthesis and translocation to the outer leaflet of the bacterial membrane are achieved by the membrane protein MprF. Consequently, mutants lacking a functional *mprF* gene are in particular vulnerable to the action of AMPs. Hence, we aim at elucidating whether and to which extent lysyl-PG modulates membrane binding, insertion, and permeabilization by various AMPs. Lysyl-PG was incorporated into artificial lipid bilayers, mimicking the cytoplasmic membrane of *S. aureus*. Moreover, we determined the activity of the peptides against a clinical isolate of *S. aureus* strain SA113 and two mutants lacking a functional *mprF* gene and visualized peptide-induced ultrastructural changes of bacteria by transmission electron microscopy. The studied peptides were: (i) NK-2, an α-helical fragment of mammalian NK-lysin, (ii) arenicin-1, a lugworm β-sheet peptide, and (iii) bee venom melittin. Biophysical data obtained by FRET spectroscopy, Fourier transform infrared spectroscopy, and electrical measurements with planar lipid bilayers were correlated with the biological activities of the peptides. They strongly support the hypothesis that peptide-membrane interactions are a prerequisite for eradication of *S. aureus*. However, degree and mode of modulation of membrane properties such as fluidity, capacitance, and conductivity were unique for each of the peptides. Altogether, our data support and underline the significance of lysyl-PG for *S. aureus* resistance to AMPs.

Antimicrobial peptides (AMPs)[2] are part of the innate immunity and provide the first line of defense against pathogenic microorganisms (1). They have a positive net charge, are 20–40 amino acid residues in length, and exhibit an amphipathic secondary structure. These features enable the interaction and permeabilization of bacterial membranes. The disturbance of the bacterial membrane may be the lethal hit itself or may allow the entrance of the peptides to reach secondary intracellular targets (2). Due to their unique mode of action, AMPs have gained high interest as new drugs to overcome bacterial resistance to classical antibiotics (3). The primary target of AMPs is the cell membrane of bacteria. It is widely accepted that the negatively charged bacterial surface plays a major role in the attraction of the cationic peptides. Biophysical studies demonstrated explicitly that model membranes consisting of anionic lipids, such as phosphatidylglycerol (PG), are particularly vulnerable to AMPs, whereas membranes of the eukaryotic zwitterionic phospholipid lecithin (phosphatidylcholine) are refractory to the peptides (4, 5). Indeed, model membranes, if their compositions really reflect those of biological membranes, can be powerful tools to unravel molecular principles of peptide-membrane interactions (6–10) and to explain the molecular basis for bacterial sensitivity and resistance to AMPs (11–13).

The opportunistic pathogen *Staphylococcus aureus* is among the bacteria that are difficult to treat, particularly by cationic antibiotics and AMPs (14, 15). This has been attributed partially to the modification of PG in the cytoplasmic membrane of *S. aureus* by the addition of a L-lysine residue, leading to lysyl-phosphatidylglycerol (lysyl-PG) (14). This reaction modifies the net charge of PG from −1 to +1 and hence should impair the initial electrostatic interaction of the cationic peptides with the bacterial membrane. The lipid portion of the cytoplasmic membrane of *S. aureus* is composed of PG and cardiolipin (16, 17), and it has been estimated that one-third of PG in the membrane is modified by lysine. PG lysinylation is achieved by the membrane protein multiple peptide resistance factor (MprF), which consists of a lysyl-PG synthase domain (18) transferring lysine from lysyl-tRNA to PG and a lysyl-PG translocase, which facilitates flipping of lysyl-PG to the outer membrane leaflet (19).

* This work was supported by Deutsche Forschungsgemeinschaft Grants SFB617 A17 and GU 568/4-1 (to T. G.), AN301/5-1 (to J. A.), and SFB766 (to A. P.).

[1] To whom correspondence should be addressed: Division of Biophysics, Research Center Borstel, Leibniz-Center for Medicine and Biosciences, Parkallee 10, D-23845 Borstel, Germany. Tel.: 49-4537-188280; Fax: 49-4537-188632; E-mail: jandrae@fz-borstel.de.

[2] The abbreviations used are: AMP, antimicrobial peptide; Ar-1, arenicin-1; DPPG, dipalmitoylphosphatidylglycerol; DOPG, dioleoyl-PG; PG, phosphatidylglycerol; FTIR, Fourier transform infrared; MIC, minimal inhibitory concentration; MprF, multiple peptide resistance factor; NBD, *N*-(7-nitrobenz-2-oxa-1,3-diazol-4yl); PE, phosphatidylethanolamine.

S. aureus strains with deletion or mutations in the *mprF* gene exhibited an attenuated virulence and were more sensitive to the action of various antimicrobial peptides such as human α-defensin HNP-1, protegrins, tachyplesin 1, nisin, magainin-2-amide (14), human β-defensin-3, and human cathelicidin LL-37 (15) but also to positively charged antibiotics such as gentamicin (15). Interestingly, *mprF* also plays a significant role in the induction of clinically relevant daptomycin resistance of methicillin-resistant *S. aureus* (MRSA) (20). The same mechanism has also been found in other bacterial pathogens. A mutant strain of *Bacillus anthracis* with the deletion of a homologue gene to *mprF* was rendered highly susceptible to the cationic peptides protamine, LL-37, and HNP-1 (21).

Despite the significance of MprF-mediated resistance of *S. aureus* to AMPs and the fact that its mechanism involves the modification of a membrane lipid, up to now, information about artificial membranes containing lysyl-PG (or a chemically related substitute) and their interaction with AMPs is very scarce. Danner *et al.* (22) described the physico-chemical properties of the pure lipid lysyl-DPPG. To study the interaction of AMPs with membranes, octadecylamine has been used as a mimetic for lysyl-PG (23), and very recently, surface association and membrane permeabilization by a synthetic peptide modeled on the basis of mammalian platelet factor 4 with liposomes comprising lysyl-PG have been investigated (24).

Here we aim at elucidating the significance and effects of a partial substitution of PG by lysyl-PG in model membranes, to mimic the cytoplasmic membrane of bacterial strains expressing or lacking the functional MprF protein, on the interaction with representative AMPs. The studied peptides were well characterized and exhibit profound activities against a clinical isolate of *S. aureus* (see Table 1). They represent three different classes of AMPs regarding structure and target selectivity. (i) Peptide NK-2 is an internal fragment of mammalian NK-lysin. It is active against Gram-negative and Gram-positive bacteria but rather non-toxic to human cells (25, 26). NK11 is an almost inactive shortened variant of NK-2 and serves as an inactive control peptide (26). Substitution of the non-functional cysteine residue of NK-2 at position 7 by a serine (C7S, NK27) or alanine residue (C7A) was performed to reduce sensitivity of the peptide to oxidation while maintaining its overall structural and physico-chemical properties. Peptide C7S was formerly referred to as NK27 (26). (ii) Arenicin-1 is a β-sheet peptide that has been isolated from immune cells of the lugworm (27). Its N and C termini are linked via an intramolecular disulfide bond. Arenicin-1 exhibits outstanding activity against Gram-negative and Gram-positive bacteria. It is non-hemolytic and very stable against tryptic digest. Moreover, it is particularly insensitive toward high salt concentration (10, 28). In addition to the natural peptide, we used a linear form where two terminal cysteine residues have been replaced by serine (C/S-Ar-1) (28). (iii) Melittin is an α-helical hemolytic peptide from bee venom (29). It has broad spectrum activity without pronounced selectivity against bacteria, fungi, and human cells and has been intensively studied by us and other groups (25, 26, 30–34).

To elucidate different aspects of peptide-membrane interactions, we performed Förster resonance energy transfer (FRET) spectroscopy to monitor insertion of the peptides into the lipid bilayer of liposomes, Fourier transform infrared (FTIR) spectroscopy to determine the fluidity and the phase transition of lipids, and Montal-Mueller planar lipid bilayers to investigate peptide binding and pore formation in membranes. Biophysical data were then correlated with the capability of the peptides to affect the viability and structural integrity of a clinical isolate of *S. aureus* (35) and of wild type SA113 as well as of two SA113-derived strains lacking a functional *mprF* gene (19).

EXPERIMENTAL PROCEDURES

Peptides—Peptides were synthesized either with a free carboxyl group or with an amidated C terminus by the Fmoc (*N*-(9-fluorenyl)methoxycarbonyl) solid-phase peptide synthesis technique on an automatic peptide synthesizer (model 433 A; Applied Biosystems) as described previously (28, 36). Disulfide linkage of terminal cysteine residues was performed in dimethyl sulfoxide (DMSO) as described (28). Peptide stocks (1 mM) in 0.01% TFA were stored at −20 °C.

Lipids and Reagents—Synthetic phospholipids 1,2-dipalmitoyl-*sn*-glycero-3-phospho-(1′-*rac*-glycerol) (DPPG), 1,2-dipalmitoyl-*sn*-glycero-3-[phospho-*rac*-(3-lysyl(1-glycerol))] (lysyl-DPPG), 1,2-dioleoyl-*sn*-glycero-3-phospho-(1′-*rac*-glycerol) (DOPG), and 1,2-dioleoyl-*sn*-glycero-3-[phospho-*rac*-(3-lysyl(1-glycerol))] (lysyl-DOPG), as well as natural L-α-phosphatidylethanolamine (PE) and L-α-phosphatidylglycerol (PG), both from *Escherichia coli* were purchased from Avanti Polar Lipids (Alabaster, AL). Fluorescently labeled phospholipids *N*-(7-nitrobenz-2-oxa-1,3-diazol-4yl)-phosphatidylethanolamine (NBD-PE) and *N*-(lissamine rhodamine B sulfonyl)-phosphatidylethanolamine (rhodamine-PE) were from Molecular Probes (Eugene, OR). Lipid stock solutions were prepared in chloroform. All lysyl-PG solutions were used immediately.

S. aureus Strains—We used a clinical isolate of *S. aureus* (35), as well as wild type SA113 (ATCC 35556), a SA113-derived strain lacking the complete *mprF* gene (Δ*mprF*), and one ΔmprF-derived strain expressing only the synthase domain of MprF but lacking the translocase domain (Δ*mprFpRBsyn*) (19). Bacteria were grown overnight in Luria-Bertani (LB) medium (Merck, Darmstadt, Germany) composed of 1% Tryptone, 0.5% yeast extract, and 1% NaCl under constant shaking at 37 °C and subsequently inoculated in the same medium to reach the mid-exponential phase.

Assay for Antibacterial Activity—Peptides were diluted from stock solutions at the desired concentration in assay buffer (20 mM HEPES, pH 7.0, with or without an additional 150 mM NaCl), and 180 μl of these solutions were filled into the wells of the first row of a microtiter plate. For a 2-fold serial dilution, 90 μl of each peptide solution were transferred to the well in the next row, which was filled with 90 μl of buffer before. Subsequently, a suspension of exponential phase bacteria in LB was added (10 μl, containing 10^4 cfu) to the peptide solution (90 μl). The constantly shaken plates were incubated in a wet chamber overnight at 37 °C. Bacterial growth was monitored by measuring the optical density at 620 nm in a microtiter plate reader (Rainbow, Tecan, Crailsham, Germany). The minimal inhibitory concentration (MIC) was defined as the lowest peptide concentration at which no bacterial growth was measurable.

Portions of each well (10 μl) were diluted with buffer and plated out in duplicates on LB-agar plates. After incubation overnight at 37 °C, bacterial colonies were counted. The minimal bactericidal concentration was defined as the lowest peptide concentration at which no colony growth was observed.

Electron Microscopy—Transmission electron microscopy was performed as described previously in detail (26). Bacteria (5×10^8 cfu/ml) were incubated with indicated concentrations of peptides in buffer (20 mM HEPES, 150 mM NaCl, pH 7.0) supplemented with 10% LB medium for 30 min at 37 °C. Images shown are representative for the respective sample.

Preparation of Liposomes for FTIR and FRET Measurements—Lipids dissolved in chloroform were dried under a gentle stream of nitrogen. The resulting lipid film was dispersed in buffer (see under "FRET and FTIR Spectroscopy"), sonicated for 30 min, and subjected to 3–4 temperature cycles from 4 to 60 °C with an incubation period of 30 min at each step. Lipid dispersions were stored at 4 °C overnight before use.

FRET Spectroscopy—Intercalation of peptides into liposome membranes was determined in 20 mM HEPES, 150 mM NaCl, pH 7.4, at 37 °C by FRET spectroscopy applied as a probe dilution assay (37). Peptides were added to liposomes, which were labeled with 1% of the donor NBD-PE and 1% of the acceptor rhodamine-PE. NBD excitation wavelength was 470 nm. Intercalation was monitored as the increase of the ratio of the donor fluorescence intensity I_{Donor} at 531 nm to that of the acceptor intensity $I_{Acceptor}$ at 593 nm in dependence on time. This ratio depends on the Förster efficiency; therefore, a rising value means that the mean distance separation of donor and acceptor dyes is rising.

FTIR Spectroscopy—The infrared spectroscopic measurements were performed on an IFS-55 spectrometer (Bruker). Pure lipids dispersed in 20 mM HEPES buffer, pH 7.0, as well as lipids mixed with peptides solubilized in the same buffer in a molar ratio of 1:0.3, were placed in a CaF_2 cuvette with a 12.5-μm Teflon spacer. Consecutive heating and cooling scans were performed automatically between 10 and 70 °C with a heating rate of 0.6 °C/min. Every 3 °C, 50 interferograms were accumulated, apodized, Fourier transformed, and converted to absorbance spectra. The peak position of the asymmetric methylene stretching vibration was plotted *versus* temperature. Phase transition temperatures were derived by determination of the maximum (minimum) of the first derivative of the heating (cooling) scans.

Preparation of Planar Bilayers and Electrical Measurements—Planar bilayers were prepared according to the Montal-Mueller technique (38) as described earlier (39). Briefly, symmetric and asymmetric bilayers were formed by opposing two lipid monolayers, prepared in separated compartments on aqueous subphases from chloroformic solutions of the lipids, at a small aperture (~150 μm) in a thin Teflon septum (thickness 25 μm). The inner leaflet of the cytoplasmic membrane of *S. aureus* was reconstituted by a phospholipid mixture consisting of an equimolar ratio of PE and PG. For electrical measurements, planar membranes were voltage-clamped via a pair of Ag/AgCl electrodes (type IVM E-255, Science Products, Hofheim, Germany) connected to the headstage of an L/M-PCA patch clamp amplifier (List-Medical, Darmstadt, Germany). In all experiments, the compartment to which peptide was added is indicated first, and the compartment opposite to the addition was grounded. In comparison with the natural system, a positive clamp voltage represents a membrane with negative potential on the inside. All measurements were performed at a temperature of 37 °C in 5 mM HEPES, 100 mM KCl, 5 mM $MgCl_2$, pH 7.0. Two electrical parameters were determined: (i) peptide-induced changes of the membrane capacitance and (ii) current through peptide-induced lesions. Assuming a plate capacitor model, the membrane capacitance yields information about the area, thickness, and composition of the bilayer. Using small positive and negative jumps of the clamp voltage, the maximum voltage required to determine membrane capacitance is <1 mV. Therefore, peptide membrane interaction can be investigated without the influence of a significant external voltage. This method allows the determination of changes in membrane capacitance with a precision of <1 picofarad. The diameter (d, nm) of pores or lesions induced by the AMPs was calculated under the assumption of a membrane of 6-nm thickness and a cylindrical pore structure using the following formula: $d = 2^*\sqrt{(L^*(6/\pi\sigma)}$, with L = measured conductivity and σ = buffer conductivity.

RESULTS

Interaction of Peptides with Intact Bacteria

Antibacterial Activity—We determined the capability of synthetic cationic peptides (Table 1) to inhibit the growth (MIC) and to kill various strains of *S. aureus* (minimal bactericidal concentration). Strains with a functional *mprF* gene, *i.e.* wild type SA113 and a clinical isolate, were considerably less sensitive to the action of the peptides. Deletion of the *mprF* gene (Δ*mprF*) rendered SA113 into a highly susceptible strain. A strain with a rescued synthase activity but still lacking the translocase domain (Δ*mprFpRBsyn*) was undistinguishable from strain Δ*mprF*, providing strong evidence that exposure of lysyl-PG to the environment is essential for conferring resistance to antimicrobial peptides. The activity of melittin was only marginally affected by the lysine modification of PG. Among the other peptides tested, arenicin was the most effective. Moreover, the activity of arenicin-1 was most strongly modulated by the expression of lysyl-PG. NK-2 was of moderate activity against strains with a functional *mprF* gene. NK11 was almost completely inactive. To elucidate the structure/function relationship of peptide NK-2 for an anti-*S. aureus* activity, we tested derivatives with the sole cysteine residue substituted by serine (C7S/NK27) or alanine (C7A) residues as well as three peptides with deletions of four adjacent residues close to the N terminus (NK23a), in the center of the molecule (NK23b), and close to the C terminus of NK-2 (NK23c). Substitution of the cysteine residue improved the activity in particular against the clinical isolate. Deletion of the central residues considerably reduced the antibacterial activity, whereas deletion of C-terminal residues led to an enhancement of activity.

Ultrastructure of Bacteria—The direct influence of peptides on the structural integrity of *S. aureus* (clinical isolate) was visualized by transmission electron microscopy (Fig. 1). More-

TABLE 1

Sequence and antibacterial activity of synthetic peptides used in this study

Peptide C7S was formerly referred to as NK27 (26). Antibacterial activity is expressed as MIC (minimal inhibitory concentration) and in MBC (minimal bactericidal concentration, shown in parantheses) in μg/ml. The NaCl concentration in the assay buffer is indicated. Ar-1, arenicin-1; -OH and -NH_2 indicate a free (carboxylated) and an amidated C terminus, respectively. Amino acid residues that are modified with respect to the lead peptide are underlined. *, >99% killing; #, data were taken from Ref. 28.

		***S. aureus* strains**							
		SA113 wt		**Δ*mprF***		**Δ*mprFpRBsyn***		**clin. isolate**	
Peptide	**Sequence**	0 mM	150 mM	0 mM	150 mM	0 mM	150 mM	0 mM	150 mM
NK-2	KILRGVCKKIMRTFLRRISKDILTGKK-NH_2	32 (256)	>256 (>256)	8 (16)	8 (16)	8 (16*)	8 (16*)	64 (128)	64 (128)
C7A	KILRGVAKKIMRTFLRRISKDILTGKK-NH_2	16 (32)	>256 (>256)	8 (32)	8 (16)	8 (16)	8 (16)	16 (32)	16 (64)
C7S/NK27	KILRGVSKKIMRTFLRRISKDILTGKK-NH_2	32 (128)	>256 (>256)	4 (16)	4 (16)	4 (8)	4 (16)	64 (128)	64 (128)
NK23a	KI SKKIMRTFLRRISKDILTGKK-NH_2	64 (128)	>256 (>256)	4 (16)	4 (8)	4 (8)	4 (8*)	32 (128*)	32 (64)
NK23b	KILRGVSKKIM RRISKDILTGKK-NH_2	256 (256)	>256 (>256)	8 (32*)	32 (64)	8 (16*)	32 (64*)	64 (256*)	128 (256*)
NK23c	KILRGVSKKIMRTFLRR ILTGKK-NH_2	32 (128)	>256 (>256)	4 (8*)	4 (32)	4 (8*)	4 (8*)	16 (64)	16 (64)
NK11	KI SK R ILTGKK-NH_2	>256 (>256)	>256 (>256)	256 (>256)	>256 (>256)	256 (>256)	256 (>256)	>256 (>256)	>256 (>256)
Melittin	GIGAVLKVLTTGLPALISWIKRKRQQ-NH_2	4 (16)	16 (64)	4 (8)	4 (4)	4 (8)	4 (8)	4 (8*)#	8 (16)#
Ar-1	RWCVYAYVRVRGVLVRYRRCW-OH	16 (64)	128 (>256)	0.5 (2)	1 (4)	0.5 (2)	2 (8*)	32 (64)#	16 (>32)#
C/S-Ar-1	RWSVYAYVRVRGVLVRYRRSW-OH	64 (256)	>256 (>256)	8 (16)	8 (16)	8 (32)	16 (32*)	128 (128*)#	32 (64*)#
R/K-Ar-1	KWCVYAYVKVKGVLVKYKKCW-OH	32 (256*)	>256 (>256)	0.5 (4)	1 (8)	0.5 (2)	4 (8*)	64 (128)#	32 (128)#

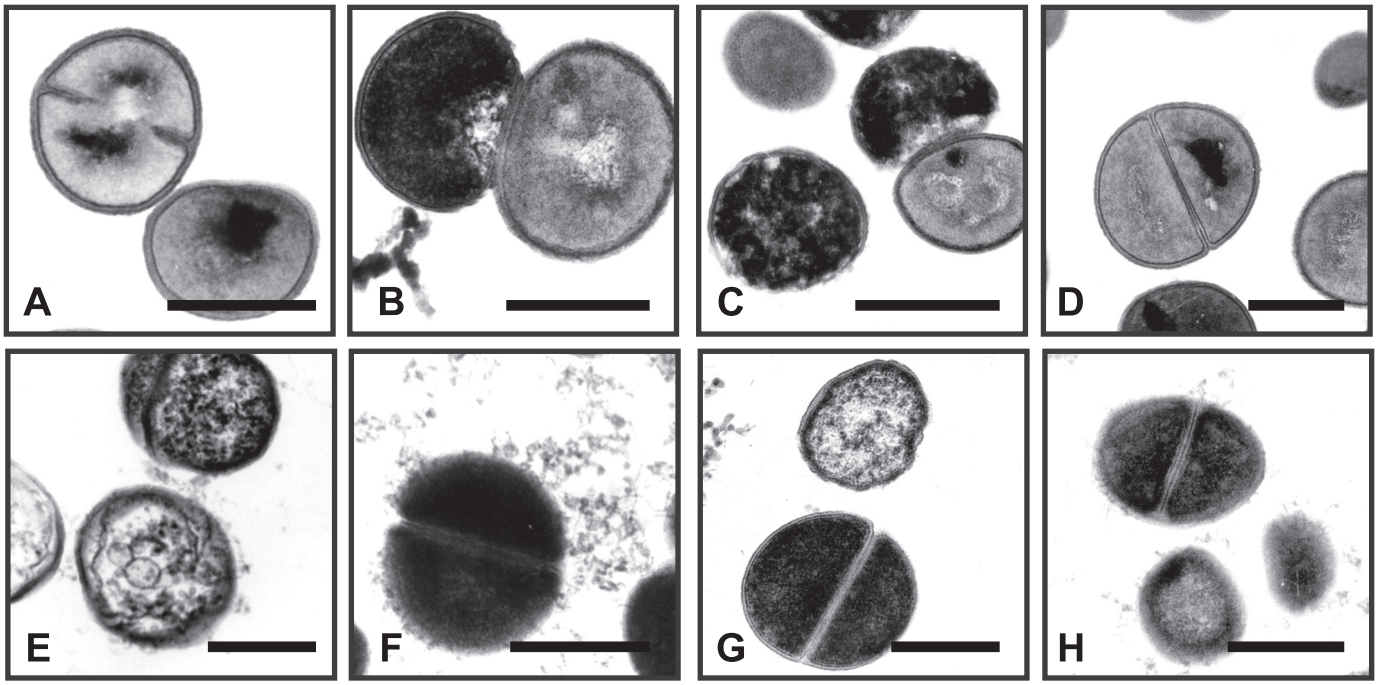

FIGURE 1. **Transmission electron microscopy images of peptide-treated *S. aureus* (clinical isolate).** *A*, no peptide. *B*, NK-2 (20 μM). *C*, C7S (20 μM). *D*, NK11 (200 μM). *E*, melittin (12 μM). *F*, Ar-1 (20 μM). *G*, C/S-Ar-1 (20 μM). *H*, R/K-Ar-1 (20 μM). Each bar represents 0.5 μm.

over, aliquots of peptide-treated bacteria were plated out on LB-agar plates, and colonies grown overnight were counted. Upon a 30-min incubation of *S. aureus* with peptides at the indicated concentrations, 80–100% of bacteria were killed, with the exception of NK11, where all bacteria survived. Peptide concentrations were chosen based on their MIC data (Table 1) to obtain a comparable killing rate. It is apparent that all peptides (except NK11, Fig. 1*D*) elicited morphological changes of *S. aureus*; however, the characteristics of structural changes were unique for each family of peptides. NK-2- and C7S-treated bacteria exhibited higher electron density in the cytoplasm than control bacteria with areas of very low electron density attached to the membrane, suggesting peptide-induced release of cytoplasmic material (Fig. 1, *B* and *C*). Bacteria incubated with melittin showed a heterogeneous electron density in the cytoplasm, and also, extracellular material emerging from the cell membrane. *S. aureus* incubated with arenicin peptides had a frayed surface (Fig. 1, *F* and *H*), an effect that was not

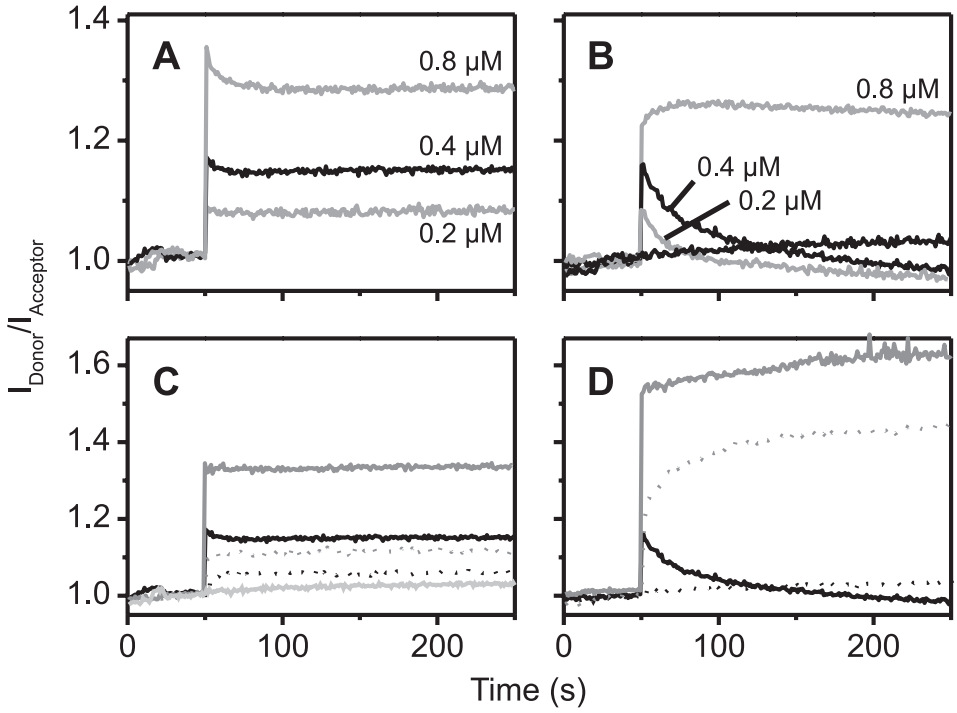

FIGURE 2. **Peptide-membrane intercalation monitored by FRET spectroscopy.** Peptides were added at 50 s. An increase of the $I_{Donor}/I_{Acceptor}$ ratio corresponded to a reduced FRET efficiency and indicated insertion of peptides into the membranes. Experiments were done in 20 mM Hepes, 150 mM NaCl, pH 7.4, at 37 °C. *A* and *B*, dose-dependent intercalation of NK-2 at the indicated concentrations with vesicles composed of DOPG (*A*) and DOPG:lysyl-DOPG (*B*). *C* and *D*, intercalation of 0.4 μM NK-2 (*solid black line*), NK11 (*dotted black line*), melittin (*solid gray line*), Ar-1 (*dotted gray line*), and control (*solid light gray line*) into liposomes made of DOPG (*C*) and DOPG:lysyl-DOPG (*D*) (50:50, by mol). For better visualization of NK11 data, the control curve has been omitted in *D*.

observed for the linear derivative C/S-Ar-1 lacking the disulfide bond (Fig. 1*G*). It appeared just as if these peptides dissolve membrane components from the bacteria or promote the release of intracellular material.

Interaction of Peptides with Artificial Membranes Composed of PG and Lysyl-PG

NK-2, melittin, Ar-1, and the most interesting derivatives were selected for an in-depth biophysical investigation with artificial membrane systems. The lipid compositions of these model systems mirrored the cytoplasmic membrane lipid composition of the various *S. aureus* strains. The membrane mimetic of wild type SA113 strain was composed of a mixture of negatively charged PG and positively charged lysyl-PG. The artificial membrane mimicking the mutant strain lacking the *mprF* gene, and thus lacking lysyl-PG in the membrane, was composed of PG alone. For the formation of planar lipid bilayers, it was necessary to dilute PG and lysyl-PG into 50% of zwitterionic PE. The fatty acid compositions of our reconstituted membranes were dictated by the respective model systems.

Membrane Intercalation of Peptides Monitored by FRET Spectroscopy—FRET spectroscopy served as a sensitive tool to detect membrane intercalation of antimicrobial peptides. For this, peptides were added to liposomes consisting of DOPG alone (Fig. 2, *A* and *C*) and of an equimolar mixture of DOPG and lysyl-DOPG (Fig. 2, *B* and *D*). All lipid vesicles were doped with donor and acceptor dyes, peptides were added, and the emission intensities of both dyes were monitored over time. An increase of the fluorescence intensity of the donor (I_{Donor}) and a simultaneous decrease of the fluorescence intensity of the acceptor dye ($I_{Acceptor}$), *i.e.* a reduced FRET efficacy, indicated an increase in the overall mean distance between the labeled phospholipids and corresponded to an insertion of peptides into the lipid bilayer. For clarity, the $I_{Donor}/I_{Acceptor}$ ratio is shown.

Upon the addition of peptides to liposomes, we observed an immediate increase of the $I_{Donor}/I_{Acceptor}$ ratio, demonstrating a rapid interaction kinetic. Intercalation of NK-2 was pronounced into pure DOPG bilayers (Fig. 2*A*) and slightly impaired into lysyl-DOPG-containing bilayers (Fig. 2*B*). Moreover, the mixed lipid system was destabilized by the peptide, indicated by a slowly decreasing $I_{Donor}/I_{Acceptor}$ ratio for 0.2 and 0.4 μM NK-2. It is likely that NK-2 initially bound to negatively charged PG, formed peptide-enriched domains, and thus excluded the dyes from these domains. NK11 interaction was significant with DOPG vesicles but negligible with liposomes containing lysyl-DOPG. A direct peptide-fluorophore interaction can be ruled out for NK-2 and peptides derived thereof by the lack of any detectable interaction with labeled phosphatidylcholine vesicles (26). Contradictory to the susceptibility tests (Table 1), the intercalation of melittin and Ar-1 was enhanced into liposome membranes containing lysyl-DOPG. Derivatives of NK-2 and Ar-1, *i.e.* C7S and C/S-Ar-1, showed an almost identical behavior as the parent peptides (data not shown).

Influence of Peptides on the Acyl Chain Fluidity of Phospholipids—The frequency of the symmetric methylene ($-CH_2-$) stretching vibration is a marker for the fluidity of the acyl chains of membrane lipids and was assessed by FTIR spec-

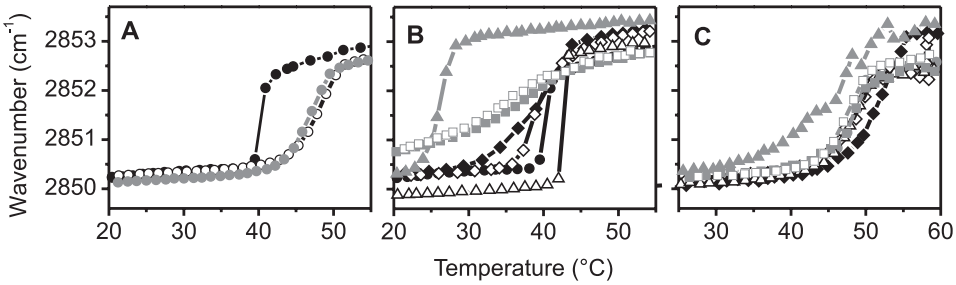

FIGURE 3. **Influence of peptides on the phase transition behavior of lipids.** The temperature dependence of the wave number of the symmetric methylene stretching vibration of the lipid acyl chains was determined by FTIR for pure lipids (*A*), for DPPG in combination with peptides (*B*), and for an equimolar mixture of DPPG:lysyl-DPPG in combination with peptides (*C*). The lipid-to-peptide molar ratio was 1:0.3. The second heating scan is shown. Lipids are as follows: DPPG (*black circles*), lysyl-DPPG (*open circles*), and DPPG:lysyl-DPPG (*gray circles*). Lipid:peptide combinations are as follows: NK-2 (*filled diamonds*), C7S (*open diamonds*), NK11 (*open triangles*), melittin (*filled triangles*), Ar-1 (*filled squares*), and C/S-Ar-1 (*open squares*).

troscopy. For this, synthetic phosphatidylglycerol (DPPG) with saturated palmitoyl chains with a defined L_β (gel) to L_α (liquid crystalline) phase transition temperature of 40–41 °C (Fig. 3*A*) has been used. For lysyl-DPPG, the phase transition temperature was broadened and shifted to 48–49 °C. A similar behavior was observed for the equimolar mixture of DPPG and lysyl-DPPG with the phase transition temperature at 46–47 °C (Fig. 3*A*). However, a pronounced hysteresis for lysyl-DPPG-containing lipid preparations has been observed, exhibiting a phase transition that was 4–5 °C lower for the cooling scan than for the heating scan (not shown). Peptides that exhibited activity against *S. aureus* destabilized the gel phase of DPPG, suggesting a disturbance of the acyl chain packing. Among them, melittin had the strongest effect. NK11, on the other hand, rigidified the gel phase and shifted the phase transition of DPPG to higher temperature, which is indicative for a superficial binding to the negatively charged lipid headgroups without penetrating the acyl chain region (Fig. 3*B*). Virtually no influence on the phase behavior of a DPPG:lysyl-DPPG mixture was observed for C7S, NK11, Ar-1, and C/S-Ar-1. Melittin had qualitatively the same effect as on the DPPG membrane; however, it was less pronounced. Peptide NK-2 behaved oppositionally on the mixed membrane by showing a stabilizing effect on the gel phase and a fluidizing effect on the liquid crystalline phase (Fig. 3*C*).

Interaction of Peptides with Planar Lipid Bilayers—The planar lipid bilayer membrane model enables the monitoring of peptide binding and peptide-induced membrane permeabilization by the measurement of membrane capacitance and resistance, respectively. For this setup, symmetric bilayers of an equimolar mixture of PG and PE (*i.e.* the reconstitution of the cytoplasmic membrane of the Δ*mprF* strain), as well as asymmetric bilayers (to mimic the wild type membrane) whose *cis* monolayer consisted of PG:lysyl-DOPG:PE (25:25:50, by mol) and whose *trans* monolayer consisted of PG:PE (50:50, by mol), were used. The course of a typical experiment was as follows. (i) The membrane was formed from two lipid monolayers on bathing solutions separated by a Teflon foil with a 120–140-μm aperture. (ii) If the membrane remained stable for at least 5 min, peptide was added to the *cis* side of the membrane, and membrane capacitance was monitored for a couple of minutes. (iii) A defined clamp voltage was applied, and current flow through the membrane was monitored until the membrane collapsed. An applied positive voltage complies with the natural situation (negative potential at the cytoplasmic side of the membrane) because in our setup, the *trans* chamber was grounded.

Injection of NK-2 into the bathing solution close to PG:PE membranes induced a drop-in capacitance of 17–21% and the formation of heterogeneous lesions after setting a clamp voltage of 20 mV (Fig. 4*A*). Moreover, the number of lesions accumulated over time and caused rapid membrane collapse. Contrarily, only a slight decrease of 3–5% in membrane capacitance was observed after the addition of NK-2 to the *cis* side of an asymmetric lysyl-PG-containing membrane. Membrane lesions were usually induced at higher voltages (50–100 mV), and the period until peptide-induced membrane collapse was significantly delayed (Fig. 4*B*). The characteristics of lesions, however, were indistinguishable for both types of membranes. No lesion formation was observed upon the addition of 0.5 μM NK11 to the bilayers. However, a slight decrease in capacitance of PG:PE bilayer indicated membrane binding (data not shown).

Melittin induced a pronounced decrease in capacitance and rapid permeabilization of symmetric PG:PE bilayers already at a concentration of 0.1 μM and 20 mV clamp voltage (Fig. 4*C*). In bilayers comprising lysyl-PG, an initial increase in capacitance of ~5% after the addition of melittin followed by a slow decrease back to the value before peptide addition have been observed. In contrast to other peptide-lipid systems, no significant decrease below that value was observed. Proximate to the change in capacitance, a rapid destabilization of the membrane occurred. In those experiments where the membrane remained stable, heterogeneous lesions accumulated at low clamp voltages (20 mV) until the membrane collapsed (Fig. 4*D*).

Interaction of Ar-1 with both types of membranes induced a similar pronounced decrease of membrane capacitance (6–28%), indicating that membrane binding was not significantly affected by substituting 50% of anionic PG by cationic lysyl-PG. Nevertheless, the formation of conducting lesions was impaired in the presence of lysyl-PG (Fig. 4*F*). Symmetric PG:PE membranes collapsed briefly after the addition of 0.5 μM Ar-1 and a clamp voltage of 20 mV, whereas current flow through asymmetric lysyl-PG-containing bilayers was detected at 50 mV or higher clamp voltages (Fig. 4*F*). The type of the formed lesions in these experiments was heterogeneous without defined conductivity levels. However, distinct conductivity levels, indicating defined pore structures, occurred in PG:lysyl-

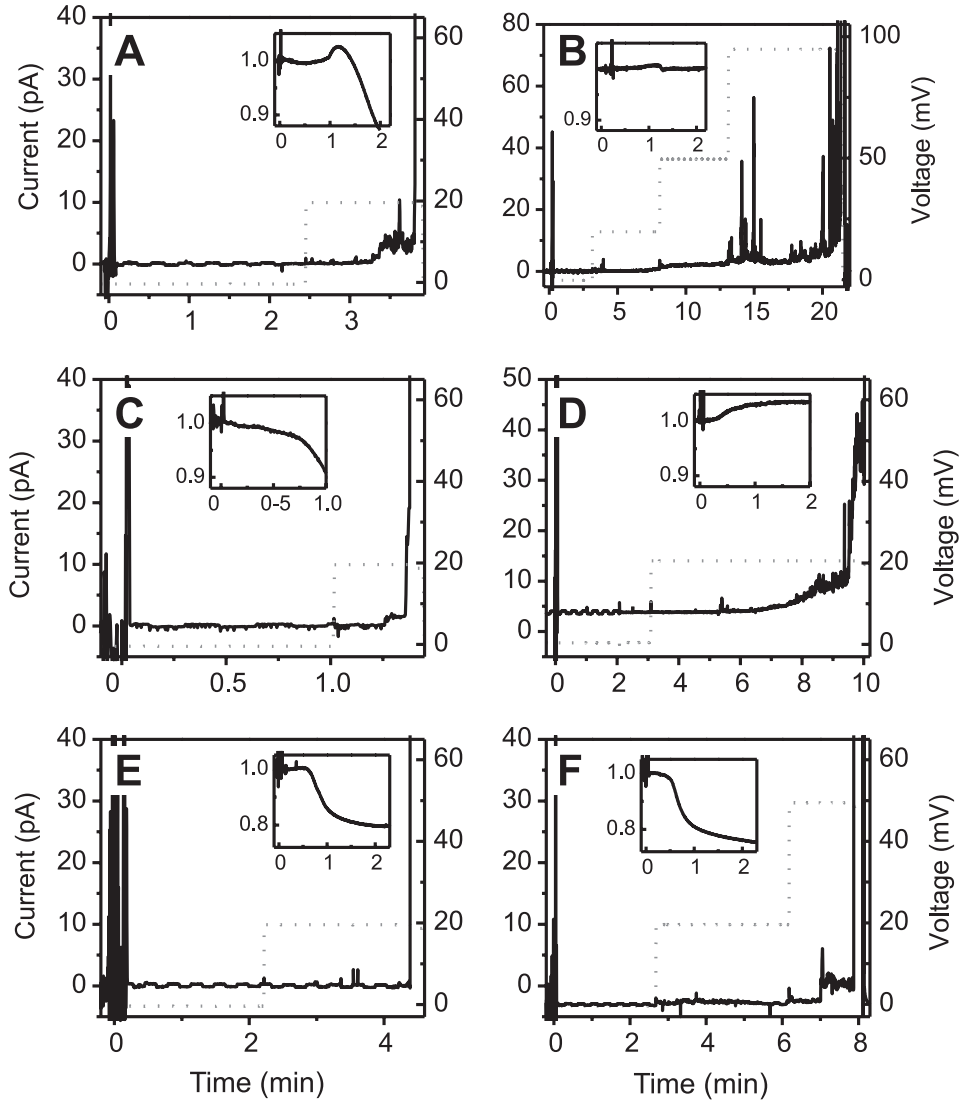

FIGURE 4. **Peptide-induced changes in membrane capacitance and current traces of planar lipid bilayers.** Peptides were added at 0 min to the *cis* side of lipid bilayers mimicking *S. aureus* Δ*mprF* mutant (PG:PE, *left column*), as well as wild type (PG:lysyl-PG:PE; *right column*) cytoplasmic membranes. *First row* (*A* and *B*), 0.5 μM NK-2. *Second row* (*C* and *D*), 0.1 μM melittin. *Third row* (*E* and *F*), 0.5 μM Ar-1. Transmembrane current and membrane capacitance (*inset*, capacitance is given as C/C_0) were monitored over time. The *trans* leaflet of each bilayer was formed of PG:PE. An applied positive voltage (*dotted line*) reflects the situation at the biological membrane (inside negative) as the *trans* side of the planar bilayer was grounded.

PG:PE membranes if the bilayer formation was done after the addition of the peptide Ar-1 to the bathing solution. The observed conductivity levels could be assigned to a basic event ($n = 1$) with a conductivity of 0.73 nanosiemens, corresponding to a pore diameter of ~0.6 nm and 2^n of the first open state ($n = 0, 1, 2, 3, \cdots$) (Fig. 5). No defined pore structures were observed for any of the other peptides under the same conditions (data not shown).

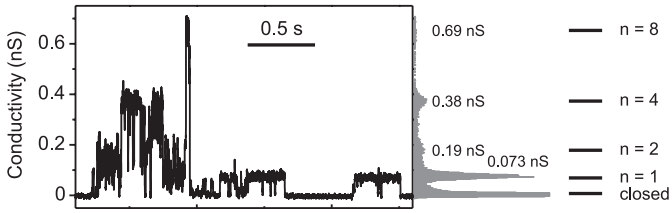

FIGURE 5. **Formation of membrane pores with defined conductivity levels by Ar-1.** An asymmetric lipid bilayer consisting of PG:lysyl-PG:PE (25:25:50) at the *cis* side and PG:PE (50:50) at the *trans* side was formed after Ar-1 (0.5 μM) had been added to the bathing solution. After setting a clamp voltage (100 mV), we observed defined conductivity levels. An applied positive voltage reflects the situation at the biological membrane (inside negative) as the *trans* side of the planar bilayer was grounded. *nS*, nanosiemens.

DISCUSSION

Deletion of the *mprF* gene in *S. aureus* strain SA113 transforms a rather refractory bacterial strain to be extremely vulnerable to peptides NK-2 and Ar-1 and to derivatives thereof. In contrast, the activity of bee venom melittin is only marginally affected. Concurrent findings with other antimicrobial peptides have been published earlier (14, 15). Beyond that, our data stress the involvement of the outer membrane leaflet exposing both cationic lysyl-PG and anionic PG to the bacterial surroundings because the origin of *mprF*-based resistance to the tested peptides was accomplished by both enzymatic activities of MprF. Rescue of the synthase activity of MprF, leading to strain Δ*mprFpRBsyn*, was insufficient to re-establish resistance. In this strain, lysyl-PG is generated but not efficiently translo-

cated to the outer membrane leaflet (19). Hence, Δ*mprFpRBsyn* exposes a predominantly negatively charged surface. Based on these findings, it appeared important to investigate the contribution of a lysyl-PG mixture in lipid bilayers for peptide-membrane interactions. Apart from whole bacteria, reconstituted membranes constitute well defined systems. They permit the application of biophysical techniques to explore the underlying molecular principles of the interplay between the (reconstituted) bacterial surface and the applied antibacterial compound, *i.e.* the peptides.

Here we successfully applied model membranes composed of distinct mixtures of PG and lysyl-PG to mimic the cytoplasmic membranes of *S. aureus* strains differing in the expression of functional MprF protein and, for the first time, analyzed the modulation of their physico-chemical properties by several cationic peptides. Complete omission of lysyl-PG from the reconstituted membranes, which would correspond to the deletion of the *mprF* gene in bacteria, dramatically influenced peptide-membrane intercalation, peptide-mediated changes of the acyl chain order (phase transition and fluidity), as well as peptide-induced membrane permeabilization by the formation of (mostly) heterogeneous lesions and changes in membrane capacitance. Altogether, our data support and underline the significance of lysyl-PG for *S. aureus* resistance to AMPs and conclusively explain MprF dependence of the anti-*Staphylococci* activity of the tested peptides by a modulated membrane interaction. However, the degree and mode of membrane modulation were unique for each of the peptides, suggesting a unique mechanism of membrane perturbation by each of the compounds. This suggestion is also supported by the elucidation of unique changes in *S. aureus* ultrastructure by each of the peptides shown in this study and by peptide-specific effects on the morphology of *Proteus mirabilis* treated with NK-2 and arenicin-1 (13, 28).

In accordance with our data, the following scenarios can be deduced for the influence of lysyl-PG in reconstituted membranes and its interaction with cationic peptides. (i) Membrane binding, intercalation, and eventually formation of membrane lesions by the peptide NK-2, which occurred in PG membranes, were considerably impaired in membranes comprising lysyl-PG. Actually, NK-2-induced lesions were a result of deep penetration of the peptide into the hydrophobic core of the bilayer formed by PG. This is indicated by a pronounced drop in FRET efficiency (*i.e.* an increase of the $I_{Donor}/I_{Acceptor}$ ratio) and in particular by a decrease (fluidizing effect) of the acyl chain order of PG, as assessed by FTIR spectroscopy. On the other hand, NK-2 increased the acyl chain order of bilayer comprising with liposomes lysyl-PG (rigidifying effect), which is likely to result from a superficial binding of cationic peptides to the membrane, thereby bridging anionic lipid head groups. In compliance with the results from FRET spectroscopy, we assume that in mixed bilayers, composed of PG and lysyl-PG, NK-2 preferentially bound to anionic PG and induced the formation of PG-enriched domains. Moreover, NK-2 placed itself into the phospholipid headgroup region, thereby increasing the mean distance between adjacent lipid molecules but without penetrating the acyl chain region. NK11, the shortened and biologically inactive derivative of NK-2, bound superficially to PG bilayers. Interaction was still detectable by a slight decrease in membrane capacitance; however, the peptide did not cause formation of any lesions or pores. (ii) Unlike NK-2, membrane binding (change in bilayer capacitance) and intercalation of Ar-1 (and partially also C/S-Ar-1) were not affected by the presence of lysyl-PG. However, subsequent membrane permeabilization was considerably impaired. This observation is in line with a recent study in which permeabilization but not binding of a synthetic peptide to membranes comprising lysyl-PG was attenuated (24). Reduced killing of *S. aureus* by the Arg to Lys substitution mutant of Ar-1 (R/K-Ar-1) indicated the significance of arginine residues to compensate for a reduced electrostatic attraction of the lysyl-PG-exposing bacterial surface. (iii) In contrast to NK-2 and Ar-1, the antibacterial activity of melittin was only marginally affected by deletion of *mprF*. Consistently, bilayer intercalation, changes in membrane fluidity, and pore formation induced by melittin, although differing by degree, were qualitatively almost indistinguishable. However, time courses of bilayer capacitance upon melittin interaction differed considerably for the wild type *S. aureus* and Δ*mprF* mutant membrane mimetics.

The applied clamp voltages used in the electrical measurements with planar lipid bilayers were actually below the natural transmembrane potential of *S. aureus*, for which values from −120 to −143 mV have been reported (40–42). Hence, herein observed voltage-dependent formation of membrane lesions is also likely to occur at the cytoplasmic membrane of live bacteria.

Peptide concentrations that induce pore formation in artificial membranes were far below the respective MIC values. To give an example, the MIC of NK-2 against strain Δ*mprF* was 8 μM, and membrane permeabilization was observed already at 0.5 μM NK-2. In other cases, this was even more dramatic. The simplest explanation for the phenomena is that the formation of a small number of lesions that can be generated in artificial bilayers by a very low concentration of peptide is not sufficient to eradicate 100% of bacteria, and thus effects are not visible in our *in vitro* assay. Furthermore, the lipid-to-peptide ratio in the two referred experiments is not comparable. It may also provide evidence for speculation that membrane permeabilization is not sufficient for killing and additional peptide molecules are required beyond mere membrane interaction (2, 43). Moreover, other factors, such as membrane proteins, lipoteichoic acids, carotenoid, and lipid II could constrain the access of peptides to the cytoplasmic membrane or affect membrane interaction. It has been shown very recently that carotenoid content of the cytoplasmic membrane affects susceptibility of *S. aureus* to certain AMPs probably by reduction of membrane fluidity (44). Lipid II, a precursor for cell wall synthesis, is used as a receptor for membrane binding and subsequent permeabilization by certain antimicrobial peptides termed lantibiotics (8, 9). It is tempting to speculate that the balance between lipid II and lysyl-PG fine-tunes the efficacy of those peptides against *S. aureus*.

The membrane model we utilized to imitate the cytoplasmic membrane of *S. aureus* strains differing in the expression of functional MprF protein was simple. However, the observed membrane modulations sufficiently explain the biological

activities of various antimicrobial peptides on the bacteria, thus emphasizing the power of reconstituted model membranes to decipher the mode of action of membrane-interacting compounds.

Moreover, the pharmaceutical potential of our peptides is highlighted by the successful design of a shortened NK-2 variant (NK23c) with an improved activity against SA113 strains and a clinically isolated *S. aureus* strain. This promising result encourages the development of short peptides for a therapeutic application.

Acknowledgments—We thank Rainer Bartels and Volker Grote for peptide synthesis, Nina Hahlbrock for FTIR measurements, Christine Hamann for FRET spectroscopy, Jasmin Tiebach for electron microscopy, and Kerstin Stephan for performing the antibacterial tests.

REFERENCES

1. Zasloff, M. (2002) *Nature* **415,** 389–395
2. Brogden, K. A. (2005) *Nat. Rev. Microbiol.* **3,** 238–250
3. Hancock, R. E., and Sahl, H. G. (2006) *Nat. Biotechnol.* **24,** 1551–1557
4. Matsuzaki, K., Sugishita, K., Fujii, N., and Miyajima, K. (1995) *Biochemistry* **34,** 3423–3429
5. Schröder-Borm, H., Willumeit, R., Brandenburg, K., and Andrä, J. (2003) *Biochim. Biophys. Acta* **1612,** 164–171
6. Shai, Y. (2002) *Biopolymers* **66,** 236–248
7. Yang, L., Harroun, T. A., Weiss, T. M., Ding, L., and Huang, H. W. (2001) *Biophys. J.* **81,** 1475–1485
8. Wiedemann, I., Böttiger, T., Bonelli, R. R., Wiese, A., Hagge, S. O., Gutsmann, T., Seydel, U., Deegan, L., Hill, C., Ross, P., and Sahl, H. G. (2006) *Mol. Microbiol.* **61,** 285–296
9. Christ, K., Wiedemann, I., Bakowsky, U., Sahl, H. G., and Bendas, G. (2007) *Biochim. Biophys. Acta* **1768,** 694–704
10. Andrä, J., Jakovkin, I., Grötzinger, J., Hecht, O., Krasnosdembskaya, A. D., Goldmann, T., Gutsmann, T., and Leippe, M. (2008) *Biochem. J.* **410,** 113–122
11. Gutsmann, T., Hagge, S. O., David, A., Roes, S., Böhling, A., Hammer, M. U., and Seydel, U. (2005) *J. Endotoxin Res.* **11,** 167–173
12. Böhling, A., Hagge, S. O., Roes, S., Podschun, R., Sahly, H., Harder, J., Schröder, J. M., Grötzinger, J., Seydel, U., and Gutsmann, T. (2006) *Biochemistry* **45,** 5663–5670
13. Hammer, M. U., Brauser, A., Olak, C., Brezesinski, G., Goldmann, T., Gutsmann, T., and Andrä, J. (2010) *Biochem. J.* **427,** 477–488
14. Peschel, A., Jack, R. W., Otto, M., Collins, L. V., Staubitz, P., Nicholson, G., Kalbacher, H., Nieuwenhuizen, W. F., Jung, G., Tarkowski, A., van Kessel, K. P., and van Strijp, J. A. (2001) *J. Exp. Med.* **193,** 1067–1076
15. Nishi, H., Komatsuzawa, H., Fujiwara, T., McCallum, N., and Sugai, M. (2004) *Antimicrob. Agents Chemother.* **48,** 4800–4807
16. Ward, J. B., and Perkins, H. R. (1968) *Biochem. J.* **106,** 391–400
17. Short, S. A., and White, D. C. (1971) *J. Bacteriol.* **108,** 219–226
18. Staubitz, P., Neumann, H., Schneider, T., Wiedemann, I., and Peschel, A. (2004) *FEMS Microbiol. Lett.* **231,** 67–71
19. Ernst, C. M., Staubitz, P., Mishra, N. N., Yang, S. J., Hornig, G., Kalbacher, H., Bayer, A. S., Kraus, D., and Peschel, A. (2009) *PLoS Pathog.* **5,** e1000660
20. Mishra, N. N., Yang, S. J., Sawa, A., Rubio, A., Nast, C. C., Yeaman, M. R., and Bayer, A. S. (2009) *Antimicrob. Agents Chemother.* **53,** 2312–2318
21. Samant, S., Hsu, F. F., Neyfakh, A. A., and Lee, H. (2009) *J. Bacteriol.* **191,** 1311–1319
22. Danner, S., Pabst, G., Lohner, K., and Hickel, A. (2008) *Biophys. J.* **94,** 2150–2159
23. Xiong, Y. Q., Mukhopadhyay, K., Yeaman, M. R., Adler-Moore, J., and Bayer, A. S. (2005) *Antimicrob. Agents Chemother.* **49,** 3114–3121
24. Kilelee, E., Pokorny, A., Yeaman, M. R., and Bayer, A. S. (2010) *Antimicrob. Agents Chemother.* **54,** 4476–4479
25. Andrä, J., and Leippe, M. (1999) *Med. Microbiol. Immunol.* **188,** 117–124
26. Andrä, J., Monreal, D., Martinez de Tejada, G., Olak, C., Brezesinski, G., Sanchez Gomez, S., Goldmann, T., Bartels, R., Brandenburg, K., and Moriyon, I. (2007) *J. Biol. Chem.* **282,** 14719–14728
27. Ovchinnikova, T. V., Aleshina, G. M., Balandin, S. V., Krasnosdembskaya, A. D., Markelov, M. L., Frolova, E. I., Leonova, Y. F., Tagaev, A. A., Krasnodembsky, E. G., and Kokryakov, V. N. (2004) *FEBS Lett.* **577,** 209–214
28. Andrä, J., Hammer, M. U., Grötzinger, J., Jakovkin, I., Lindner, B., Vollmer, E., Fedders, H., Leippe, M., and Gutsmann, T. (2009) *Biol. Chem.* **390,** 337–349
29. Habermann, E., and Jentsch, J. (1967) *Hoppe-Seyler's Z. Physiol. Chem.* **348,** 37–50
30. Blondelle, S. E., and Houghten, R. A. (1991) *Biochemistry* **30,** 4671–4678
31. Werkmeister, J. A., Kirkpatrick, A., McKenzie, J. A., and Rivett, D. E. (1993) *Biochim. Biophys. Acta* **1157,** 50–54
32. Andrä, J., Berninghausen, O., Wülfken, J., and Leippe, M. (1996) *FEBS Lett.* **385,** 96–100
33. Russell, P. J., Hewish, D., Carter, T., Sterling-Levis, K., Ow, K., Hattarki, M., Doughty, L., Guthrie, R., Shapira, D., Molloy, P. L., Werkmeister, J. A., and Kortt, A. A. (2004) *Cancer Immunol. Immunother.* **53,** 411–421
34. Schröder-Borm, H., Bakalova, R., and Andrä, J. (2005) *FEBS Lett.* **579,** 6128–6134
35. Leippe, M., Andrä, J., and Müller-Eberhard, H. J. (1994) *Proc. Natl. Acad. Sci. U.S.A.* **91,** 2602–2606
36. Andrä, J., Koch, M. H., Bartels, R., and Brandenburg, K. (2004) *Antimicrob. Agents Chemother.* **48,** 1593–1599
37. Schromm, A. B., Brandenburg, K., Rietschel, E. T., Flad, H. D., Carroll, S. F., and Seydel, U. (1996) *FEBS Lett.* **399,** 267–271
38. Montal, M., and Mueller, P. (1972) *Proc. Natl. Acad. Sci. U.S.A.* **69,** 3561–3566
39. Wiese, A., and Seydel, U. (2000) *Methods Mol. Biol.* **145,** 355–370
40. Collins, S. H., and Hamilton, W. A. (1976) *J. Bacteriol.* **126,** 1224–1231
41. Koo, S. P., Bayer, A. S., Sahl, H. G., Proctor, R. A., and Yeaman, M. R. (1996) *Infect. Immun.* **64,** 1070–1074
42. Pag, U., Oedenkoven, M., Papo, N., Oren, Z., Shai, Y., and Sahl, H. G. (2004) *J. Antimicrob. Chemother.* **53,** 230–239
43. Hale, J. D., and Hancock, R. E. (2007) *Expert Rev. Anti Infect. Ther.* **5,** 951–959
44. Mishra, N. N., Liu, G. Y., Yeaman, M. R., Nast, C. C., Proctor, R. A., McKinnell, J., and Bayer, A. S. (2011) *Antimicrob. Agents Chemother.* **55,** 526–531